

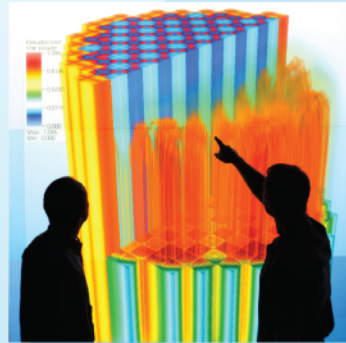


Power updates
and plant life extension

CASL-U-2013-0223-000



Consortium for Advanced Simulation of LWRs



Engineering design
and analysis

L3:VUQ.SAUQ.P6.01 Milestone Report - A Comparison of Adjoint and Data-Centric Verification Techniques

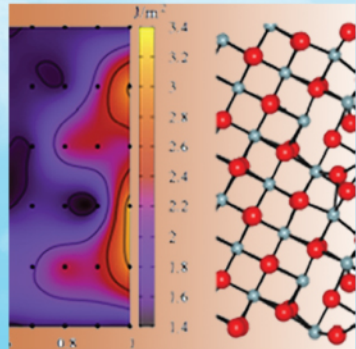
T.M. Wildey, E.C. Cyr, J.N. Shadid, R.
Pawlowski, T. Smith

Sandia National Laboratory

March 2014



Science-enabling
high performance
computing



Fundamental science



Plant operational data



U.S. DEPARTMENT OF

ENERGY

Nuclear Energy

SANDIA REPORT

2013-2879
Unlimited Release
Printed March 2013

A Comparison of Adjoint and Data-Centric Verification Techniques

Timothy M. Wildey, Eric C. Cyr, John N. Shadid, Roger Pawlowski, Tom Smith.

Prepared by
Sandia National Laboratories
Albuquerque, New Mexico 87185 and Livermore, California 94550

Sandia National Laboratories is a multi-program laboratory managed and operated by Sandia Corporation, a wholly owned subsidiary of Lockheed Martin Corporation, for the U.S. Department of Energy's National Nuclear Security Administration under contract DE-AC04-94AL85000.

Approved for public release; further dissemination unlimited.



Sandia National Laboratories

Issued by Sandia National Laboratories, operated for the United States Department of Energy by Sandia Corporation.

NOTICE: This report was prepared as an account of work sponsored by an agency of the United States Government. Neither the United States Government, nor any agency thereof, nor any of their employees, nor any of their contractors, subcontractors, or their employees, make any warranty, express or implied, or assume any legal liability or responsibility for the accuracy, completeness, or usefulness of any information, apparatus, product, or process disclosed, or represent that its use would not infringe privately owned rights. Reference herein to any specific commercial product, process, or service by trade name, trademark, manufacturer, or otherwise, does not necessarily constitute or imply its endorsement, recommendation, or favoring by the United States Government, any agency thereof, or any of their contractors or subcontractors. The views and opinions expressed herein do not necessarily state or reflect those of the United States Government, any agency thereof, or any of their contractors.

Printed in the United States of America. This report has been reproduced directly from the best available copy.

Available to DOE and DOE contractors from
U.S. Department of Energy
Office of Scientific and Technical Information
P.O. Box 62
Oak Ridge, TN 37831

Telephone: (865) 576-8401
Facsimile: (865) 576-5728
E-Mail: reports@adonis.osti.gov
Online ordering: <http://www.osti.gov/bridge>

Available to the public from
U.S. Department of Commerce
National Technical Information Service
5285 Port Royal Rd
Springfield, VA 22161

Telephone: (800) 553-6847
Facsimile: (703) 605-6900
E-Mail: orders@ntis.fedworld.gov
Online ordering: <http://www.ntis.gov/help/ordermethods.asp?loc=7-4-0#online>



2013-2879
Unlimited Release
Printed March 2013

A Comparison of Adjoint and Data-Centric Verification Techniques

Timothy M. Wildey,
Eric C. Cyr,
John N. Shadid,
Roger Pawlowski,
Tom Smith
Sandia National Laboratories
P.O. Box 5800
Albuquerque, NM 87185-1318
tmwilde@sandia.gov

Abstract

This document summarizes the results from a level 3 milestone study within the CASL VUQ effort. We compare the adjoint-based a posteriori error estimation approach with a recent variant of a data-centric verification technique. We provide a brief overview of each technique and then we discuss their relative advantages and disadvantages. We use Drekar::CFD to produce numerical results for steady-state Navier Stokes and SARANS approximations.

Contents

0.1	Motivation	9
0.2	Data-Centric Verification Techniques	10
0.3	Adjoint Based Error Analysis	12
0.3.1	General Nonlinear Problem and Notation	12
0.3.2	Strong Form Adjoint Operators	13
0.3.3	Variational Formulation	13
0.3.4	Accuracy of Error Estimate	14
0.3.5	Drekar Implementation	15
0.3.6	Adjoint Consistency	15
0.4	Advantages and Disadvantages	16
0.5	Computational Experiments	19
0.5.1	Navier Stokes Channel Flow	19
0.5.2	RANS Model for Axisymmetric Expansion	24
0.6	Conclusions	30
	References	31

List of Figures

1	Chart showing the relationship (or lack thereof) between the forward and adjoint operators and their respective stabilized and discrete variants.	16
2	Magnitude of the forward velocity for the channel verification problem.	20
3	Estimated convergence rates for the ensemble of regressions for Q_1 (left) and Q_2 (right).	21
4	Estimated asymptotic values for the ensemble of regressions for Q_1 (left) and Q_2 (right).	21
5	Approximate values of the quantities of interest as well as the sum of the approximations and the error estimates for Q_1 (left) and Q_2 (right).	23
6	Coarsest (left) and finest (right) computational meshes for the axisymmetric sudden expansion problem.	24
7	Estimated convergence rates for the ensemble of regressions for Q_1 (upper-left), Q_2 (upper-right), and Q_3 (lower-middle).	26
8	Estimated asymptotic values for the ensemble of regressions for Q_1 (upper-left), Q_2 (upper-right), and Q_3 (lower-middle).	27
9	Estimated convergence rates for the ensemble of regressions for Q_1 (upper-left), Q_2 (upper-right), and Q_3 (lower-middle).	29
10	Estimated asymptotic values for the ensemble of regressions for Q_1 (upper-left), Q_2 (upper-right), and Q_3 (lower-middle).	30

List of Tables

1	Values of the quantities of interest for a sequence of discretizations.	20
2	Values of the a posteriori error estimates and effectivity ratios for a sequence of discretizations.	22
3	Number of nodes and elements on each of the five meshes.	24
4	Values of the quantities of interest for a sequence of discretizations using a prescribed inflow velocity.	25
5	Values of the error estimates for a sequence of discretizations using a prescribed inflow velocity.	27
6	Values of the quantities of interest for a sequence of discretizations using a pressure drop to drive the flow.	28
7	Values of the error estimates for a sequence of discretizations using a prescribed inflow velocity.	29

0.1 Motivation

Verification is a necessary, but often neglected, process that helps to assess the predictive capabilities of a numerical simulation. While the precise definition of verification may vary between disciplines, one of the main objectives in verification is usually to determine whether or not a discretized problem is an accurate representation of a continuous system, and whether the discrete approximation converges to the continuous solution as the discretization is refined. Often, there are well-established asymptotic convergence rates for the numerical algorithms employed by the simulation. In such cases, verification usually involves solving an idealized problem, i.e., one with an analytical or manufactured solution, on a sequence of discretizations and checking whether the rate of convergence of various quantities of interest matches the theoretical rate. Unfortunately, such idealized problems often do not necessarily represent the normal operating conditions for the simulation, and therefore, may not provide a reliable assessment of its predictive capabilities.

In response to this observation, recent verification work has focused on estimating the asymptotic rate of convergence for more realistic simulations where the asymptotic value of the quantity of interest is unknown. The drawback is that several levels of refinement may be necessary to infer both the asymptotic value of the quantity of interest and the asymptotic convergence rate. Richardson extrapolation can be used to infer the asymptotic value of the quantity of interest, but this also requires three numerical approximations in the asymptotic range. Thus, recent research has focused on techniques that can provide asymptotic information and uncertainty estimates with a minimal number of simulations. The Grid Convergence Index (GCI) [18] is perhaps the first attempt to infer these asymptotic parameters from data along with an estimate of the uncertainty in the estimates. A variety of similar techniques have subsequently been developed (see e.g., [20, 16, 15] and the references therein): each using different assumptions and/or user experience to determine the appropriate *safety or correction factors* to improve the reliability of the uncertainty estimates without gross overestimation.

Tangentially, a posteriori error estimation techniques have become a common means to quantify the reliability of predictions from numerical simulations. This methodology has been developed for a large number of methods and is widely accepted in the analysis of discretization error for partial differential equations [1, 6, 7]. While many a posteriori techniques focus on estimating the error in a particular norm, such as the L^2 or the energy norm, the adjoint-based (dual-weighted residual) method, is motivated by the observation that oftentimes the goal of a simulation is to compute a small number of linear functionals of the solution, such as the average value in a region or the drag on an object, rather than controlling the error in a global norm. This method has been successfully utilized to estimate the error in quantities of interest for a class of transient nonlinear problems and has recently been extended to estimate numerical errors due to operator splittings [8] and operator decomposition for multiscale/multiphysics applications [3, 10, 11]. The a posteriori error estimation approach does not require as many simulations to infer the asymptotic values of the quantity of interest and the convergence rate, but it is also subject to accuracy concerns if the simulation is not near the asymptotic regime. Moreover, the adjoint problem can only be defined for a certain class of quantities of interest and therefore a posteriori error estimate are only available for these quantities of interest. The limitations of this approach are discussed further in section 0.4.

The goal of this report is to provide a concise discussion of the relative advantages and disadvantages of the adjoint-based and data-centric approaches to verification, and to demonstrate each of these on a set of simulations of interest to CASL. In this report, we restrict the discussion to the solution of steady-state nonlinear coupled systems of partial differential equations. The similar comparison for time-dependent problems would be of interest, but the current capabilities in Drekar::CFD do not allow for time-dependent adjoint simulations. This is work in progress and may be discussed in a future report. The remainder of this report is organized as follows. In section 0.2, we briefly describe the data-centric approach to verification and how the approach taken in [17] differs from previous approaches. In section 0.3, we describe the adjoint-based error estimation technique and discuss how the adjoint solution is approximated in Drekar::CFD. Next, in section 0.4, we compare the two approaches and give a short description of their relative advantages and disadvantages. In section 0.5, we use Drekar::CFD to compute various quantities of interest and the adjoint-based error estimates from steady state Navier Stokes and Reynolds Averaged Navier Stokes (RANS) models. Finally, some concluding remarks are presented in section 0.6.

0.2 Data-Centric Verification Techniques

In this section, we summarize the data-centric verification technique in [17] and describe how this technique differs from previous approaches, e.g., [18, 20, 16, 15]. However, following [17], it is useful to start with a discussion of *error* and what assumptions can be reasonable to make. We assume that the goal of the simulation is to provide accurate estimates of quantities of interest from the following systems of partial differential equations,

$$\mathbf{F}(\mathbf{z}) = \mathbf{0}, \tag{1}$$

defined on some domain $\Omega \subset \mathbb{R}^d$. Here, \mathbf{z} is the continuous solution of the system of PDEs. We allow (1) to be nonlinear and time-dependent, but we assume that it is a deterministic problem in the sense that repeated evaluations given the same discretization, initial/boundary conditions, and model parameters (a.k.a scenario) provide the same solution. Since analytical solution of systems like (1) are rarely available, we must resort to numerical approximations of the solution. We let \mathbf{Z} denote the numerical approximation of \mathbf{z} and we use $\mathbf{e} = \mathbf{z} - \mathbf{Z}$ to denote the error.

In general, the error depends on variety of factors:

1. Spatial discretization errors (mesh size).
2. Temporal discretization errors (time-stepping).
3. Numerical quadrature errors.
4. Errors due to linear and nonlinear solver tolerances.
5. Operator splitting errors.

6. Implementation errors.
7. Errors due to inconsistencies in the discrete formulation.
8. Rounding errors due to finite machine precision.
9. ...

While factors 6 and perhaps 7 can be eliminated, most are present in some amount for any numerical approximation.

We emphasize that while the error itself is unknown, it is not random and one should not assume that a probabilistic characterization is appropriate [16, 15]. This is due to the fact that all of the sources of error are completely deterministic which follows from our assumption that the model itself is deterministic. There are plenty of models that are inherently stochastic, such as models for stock prices or molecular dynamics, and for these models the error has both deterministic and stochastic contributions.

To simplify the verification process, one would prefer to consider one factor at a time by driving the other factors down to so that their contributions are negligible. This would allow one to verify that the error converges optimally with respect to each factor. In this report, we focus on the spatial discretization error and while we acknowledge that the other sources of error are present, we assume that they are negligible. This leads to the following ansatz for a quantity of interest:

$$q(\mathbf{z}) = q(\mathbf{Z}) + Ch^r + \text{higher order terms} , \quad (2)$$

where $q(\mathbf{z})$ is the true value of the quantity of interest, which is unknown, $q(\mathbf{Z})$ is the numerical approximation, h is a parameter associated with the spatial discretization, and C and r are the unknown parameters associated with the spatial discretization error. Typically, we are given a set of mesh sizes $\{h_1, h_2, \dots, h_N\}$ and a set of values of numerical approximations of the quantity of interest (data) $\{q_1, q_2, \dots, q_N\}$. The objective is then to infer the values of $q(\mathbf{z})$, C , and r from the data. One might attempt to use Richardson extrapolation to estimate $q(\mathbf{z})$, but it is usually more effective to allow the optimization scheme to find the value of $q(\mathbf{z})$ that best fits the data according to the ansatz. Similarly, one might assume that r is known based on a priori assumptions on the numerical approximation, but this is also prone to complications since the continuous solution may not have sufficient regularity to converge at the optimal rate. In our view, it is best to leave $q(\mathbf{z})$, C and r as unknown and find the values that best fit the data with respect to some metric. However, the choice of metric affects how one may interpret the results.

The standard approach is to use nonlinear least-squares to approximate the unknown parameters in (2). While this gives a reasonable approximation of the parameters, an issue arises if one chooses to use the misfit between the least squares approximation and the data to say anything about the uncertainty in the parameter approximations. The issue is described in detail in [17], but the point is that, for any regression scheme, the assumption that the misfits can be used to estimate the error in the parameter approximations relies on the assumption that the neglected terms in (2) are random variables with a particular distribution. For example, the assumed distribution is Gaussian for least squares regression. As previously mentioned (and emphasized in [17]), there is

no theoretical justification for such assumptions. Nevertheless, such approaches are quite common and have been utilized in a very large number of verification exercises.

Consequently, the novelty of the approach taken in [17] was the use of an ensemble of regressions to generate a set of estimates of the parameters and to use the median of the estimates (not the mean!) for verification purposes. The ensemble of regressions are generated using various metric on selected subsets of the data. Typically, subsets of the data are selected by starting with the values of the quantities of interest on the finest discretizations and adding the values from coarser discretizations as appropriate. In [17], a wide variety of metrics were used for regression: L^2 , L^1 , L^∞ , and a weighted L^2 where the results on finer grids are given higher weighting. The authors also considered several metrics where the convergence rate was assumed and only the asymptotic value of the quantity of interest and the constant, C , were optimized. In this report, we focus on the standard metrics: L^2 , L^1 , L^∞ , and weighted L^2 . Again, following [17], we use the median deviation to produce an estimate of the uncertainty in the asymptotic approximations rather than making a probabilistic assumption on the higher order terms in the ansatz.

0.3 Adjoint Based Error Analysis

As previously stated, the goal is adjoint-based error estimation to relate the error in a quantity of interest, which is usually not computable, to a weighted residual, which is computable. The weights on the residual are given by the solution to an appropriately defined adjoint problem. This is very similar to way in which adjoints are used in optimization and uncertainty quantification to provide sensitivity/derivative information. We remark that, in general, adjoints are not unique and basically any supplementary problem can be used to derive a representation for the error in a quantity of interest. The adjoint problem is usually defined so that all of the terms in the error representation are either computable (given an approximation of the adjoint solution) or negligible. For many problems, several different adjoints can lead to computable error representations and the choice of the adjoint problem depends mostly on the approximation properties of the adjoint solution and the ease of implementation in the simulation framework. We take a particularly straightforward approach in Drekar::CFD which we describe in section 0.3.5. For more details on the implementation of adjoint-based a posteriori error estimates in Drekar::CFD, see [19].

0.3.1 General Nonlinear Problem and Notation

We consider the following system of partial differential equations,

$$\mathbf{F}(\mathbf{z}) = \mathbf{0}, \tag{3}$$

defined on $\Omega \subset \mathbb{R}^d$, $d = 2, 3$, a polygonal (polyhedral) domain (open, bounded, and connected set) with boundary $\partial\Omega$. Specific examples of \mathbf{F} and \mathbf{z} will be given in subsequent sections. We assume that sufficient boundary conditions are provided so that (3) is well-posed. We present the definition of the adjoint problem and the a posteriori error analysis using the general problem formulation (3).

0.3.2 Strong Form Adjoint Operators

The goal in adjoint-based error analysis is to relate a linear (or linearized) functional of the error to a computable weighted residual. The linear adjoint operator in strong form can be defined via the duality relation

$$(\mathcal{L}\mathbf{v}, \mathbf{w}) = (\mathbf{v}, \mathcal{L}^*\mathbf{w}) \quad (4)$$

where \mathcal{L} is a linear operator. For a general nonlinear PDE one approach to define the linear operator \mathcal{L} is to assume \mathbf{F} is convex and use the Integral Mean Value Theorem yielding

$$\mathbf{F}'(\bar{\mathbf{z}})\mathbf{e} = \mathbf{F}(\mathbf{z}) - \mathbf{F}(\mathbf{z}_h)$$

where $\bar{\mathbf{z}}$ lies on the line connecting \mathbf{z} and \mathbf{z}_h , and $\mathbf{e} = \mathbf{z} - \mathbf{z}_h$. In practice, $\bar{\mathbf{z}}$ is unknown so we linearize around \mathbf{z}_h giving,

$$\mathcal{L}\mathbf{e} = \mathbf{F}'(\mathbf{z}_h)\mathbf{e} = \mathbf{F}(\mathbf{z}) - \mathbf{F}(\mathbf{z}_h) + h.o.t.$$

Notice that the operator \mathcal{L} is the same linear operator used in computing the step in Newton's method. This fact is often exploited to ease construction of the discrete adjoint operator.

For the linear functional denoted by the duality pairing $(\boldsymbol{\psi}, \cdot)$ the error can be represented using the definition of the adjoint. We follow the standard approach and neglect the higher order terms in the error representation, see e.g. [2, 1, 9, 11], giving

$$(\boldsymbol{\psi}, \mathbf{e}) = (\boldsymbol{\psi}, \mathcal{L}^{-1}(\mathbf{F}(\mathbf{z}) - \mathbf{F}(\mathbf{z}_h))) = (\boldsymbol{\phi}, \mathbf{F}(\mathbf{z}) - \mathbf{F}(\mathbf{z}_h)) \quad (5)$$

where $\boldsymbol{\phi}$ is defined by the adjoint problem

$$\mathcal{L}^*\boldsymbol{\phi} = \boldsymbol{\psi}. \quad (6)$$

0.3.3 Variational Formulation

We assume that (3) has an equivalent variational formulation seeking $\mathbf{z} \in \mathbf{V}$ such that,

$$\mathbf{f}(\mathbf{z}, \mathbf{w}) = \mathbf{0}, \quad \forall \mathbf{w} \in \mathbf{V}. \quad (7)$$

Note that \mathbf{f} is assumed to be linear \mathbf{w} . Specific examples of \mathbf{f} and \mathbf{V} will be given in subsequent sections. The discrete problem is defined by choosing $\mathbf{V}_h \subset \mathbf{V}$ to be a discrete subspace associated with the partition, \mathcal{T}_h , and letting $\mathbf{z}_h \in \mathbf{V}_h$ satisfy,

$$\mathbf{f}(\mathbf{z}_h, \mathbf{w}) = \mathbf{0}, \quad \forall \mathbf{w} \in \mathbf{V}_h. \quad (8)$$

This statement combined with the linearity in \mathbf{w} is equivalent to *Galerkin orthogonality*, and in what follows we will refer to these interchangeably.

Deriving the adjoint of the variational formulation follows the same pattern as the strong-form operator. To define the error representation the Integral Mean Value Theorem is again applied giving

$$\mathbf{f}'(\bar{\mathbf{z}}; \mathbf{e}, \mathbf{w}) = \mathbf{f}(\mathbf{z}, \mathbf{w}) - \mathbf{f}(\mathbf{z}_h, \mathbf{w}) \quad (9)$$

where

$$\mathbf{a}(\mathbf{z}; \mathbf{v}, \mathbf{w}) = \left. \frac{\partial}{\partial \varepsilon} \mathbf{f}(\mathbf{z} + \varepsilon \mathbf{v}, \mathbf{w}) \right|_{\varepsilon=0} = \mathbf{f}'(\mathbf{z}; \mathbf{v}, \mathbf{w}). \quad (10)$$

Again linearizing about \mathbf{z}_h and neglecting high order terms, the error in a linear functional defined by the duality pairing $(\boldsymbol{\psi}, \cdot)$ can be written as

$$(\boldsymbol{\psi}, \mathbf{e}) = \mathbf{a}(\mathbf{z}_h; \mathbf{e}, \boldsymbol{\phi}) = -\mathbf{f}(\mathbf{z}_h, \boldsymbol{\phi}) \quad (11)$$

where $\boldsymbol{\phi}$ is the solution to the adjoint problem

$$\mathbf{a}(\mathbf{z}_h; \mathbf{w}, \boldsymbol{\phi}) = (\boldsymbol{\psi}, \mathbf{w}), \quad \forall \mathbf{w} \in \mathbf{V}. \quad (12)$$

Given $\boldsymbol{\phi}$ the error representation Eq. 11 is easily evaluated. However, usually the solution to the adjoint problem Eq. 12 is not given explicitly and we must approximate the solution using an appropriate discretization. In section 0.3.4, we discuss various strategies to approximate the adjoint solution and how these approximations affect the accuracy of the adjoint-based error estimate.

0.3.4 Accuracy of Error Estimate

One of the challenges in goal-oriented a posteriori error estimation is the fact that the adjoint solution needs to be approximated using a finer discretization than was used for the forward problem. Occasionally we can use the same approximation for the forward and adjoint problems, but this requires that the adjoint solution be projected into a finer space [2, 1]. While this is appealing from a computational perspective, in general it is difficult to define such projection operators and consequently the error estimates are often inaccurate. In `Drekar::CFD`, we use piecewise linear Galerkin finite elements with SUPG stabilization to solve the forward problem and a higher-order (quadratic) finite element approximation with stabilization to solve the adjoint problem. Using a higher order approximation to solve the adjoint is generally regarded as the most robust approach to obtain accurate error estimates. The increase in computational cost associated with the higher-order basis functions is somewhat mitigated by the fact that the adjoint problem is linear.

In general, we can rewrite the error representation (11) using an approximate adjoint solution, $\tilde{\boldsymbol{\phi}} \approx \boldsymbol{\phi}$, as follows,

$$(\boldsymbol{\psi}, \mathbf{e}) = -\mathbf{f}(\mathbf{z}_h, \tilde{\boldsymbol{\phi}}) - \mathbf{f}(\mathbf{z}_h, \boldsymbol{\phi} - \tilde{\boldsymbol{\phi}}).$$

The second term is a product of the forward residual and the adjoint error. We can safely assume that the second term is negligible if the error in solving the adjoint is smaller than the error in solving the forward problem. We can actually get away with a much weaker assumption, namely, that the error in solving the adjoint is small in regions where the error in solving the forward problem is large. Stated another way, the adjoint does not need to be accurate in regions where the forward error is small. This has led to research into the use of different physical discretizations for the forward and adjoint problem, but this is beyond the scope of this paper.

0.3.5 Drekar Implementation

Drekar::CFD is a massively parallel unstructured fully-implicit (or semi-implicit) finite element Navier-Stokes solver built upon Trilinos [14]. The automatic differentiation tools allow for rapid code development and a straightforward implementation of advanced capabilities such as embedded uncertainty quantification and adjoints. We summarize the implementation of the adjoint-based error estimates in Drekar::CFD in Algorithm 0.3.5.

Algorithm 1 Computation of the a posteriori Error Estimate

Given low order and high order approximation spaces: \mathbf{V}_L and \mathbf{V}_H respectively.

Given a low order approximation of the forward solution, $\mathbf{z}_L \in \mathbf{V}_L$ satisfying

$$\mathbf{f}_\tau(\mathbf{z}_L, \mathbf{v}_L) = 0, \quad \forall \mathbf{v}_L \in \mathbf{V}_L.$$

Given a QoI defining adjoint data:

$$\boldsymbol{\psi}_H = (\boldsymbol{\psi}, \mathbf{v}_H), \quad \forall \mathbf{v}_H \in \mathbf{V}_H.$$

Project forward approximation into higher order space (usually trivial):

$$\mathcal{P}\mathbf{z}_L = \mathbf{z}_H.$$

Compute residual of forward problem in higher order space:

$$\mathbf{r}_H = -\mathbf{f}_\tau(\mathbf{z}_H, \mathbf{v}_H), \quad \forall \mathbf{v}_H \in \mathbf{V}_H.$$

Compute adjoint of Jacobian in higher order space such that:

$$\mathbf{J}_H^T \boldsymbol{\phi}_H = \mathbf{a}_\tau(\mathbf{z}_H; \mathbf{v}_H, \boldsymbol{\phi}_H), \quad \forall \mathbf{v}_H \in \mathbf{V}_H.$$

Solve the adjoint problem:

$$\mathbf{J}_H^T \boldsymbol{\phi}_H = \boldsymbol{\psi}_H.$$

Compute the error estimate as a weighted residual:

$$(\boldsymbol{\psi}, \mathbf{e}) = (\mathbf{r}_H, \boldsymbol{\phi}_H).$$

0.3.6 Adjoint Consistency

Adjoint consistency is an issue whenever the adjoint of the discretization of the forward problem does not correspond to a discretization of the formal adjoint problem. This is known to be problematic for certain adjoint inconsistent formulations, e.g. stabilized Galerkin methods [5] and interior penalty discontinuous Galerkin methods [13, 12, 5]. Often, the adjoint of the discretized system is preferred due to ease of implementation, but it has been shown that for SUPG stabilized methods

a discretization of the formal adjoint system may produce better results, see [4] for an example in an optimization setting. In Figure 1, we illustrate that there may exist an additional layer of

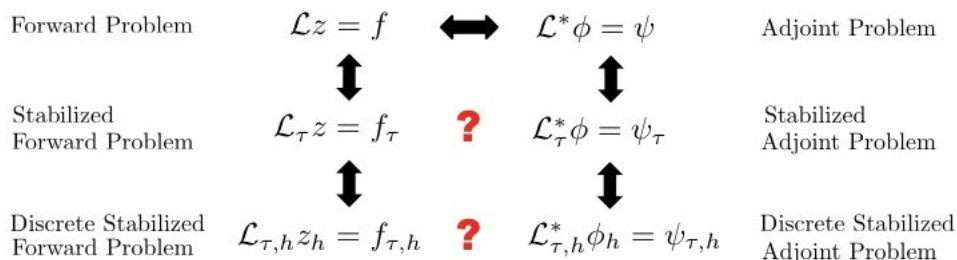


Figure 1. Chart showing the relationship (or lack thereof) between the forward and adjoint operators and their respective stabilized and discrete variants.

complexity. Namely, the problem formulation itself may be modified, usually in a consistent fashion, before discretization. Often, this modification affects both the operator and the data, and is designed to introduce additional stability in the discrete formulation, but it is not always the case that the adjoint of the modified problem corresponds to a modification of the adjoint problem. In this case, the formulation is not adjoint consistent.

The adjoint implementation in Drekar::CFD uses a *discrete adjoint*. Thus far the results have been favorable using the discrete adjoint approximation. The framework and adjoint implementation in Drekar::CFD are flexible enough to allow for an approximation of the continuous adjoint, but this has yet to be explored.

0.4 Advantages and Disadvantages

In this section, we make a number of concise statements regarding the relative advantages and disadvantages of the data-centric and adjoint-based techniques. Each statement is followed by a brief explanation. This list is by no means exhaustive, but it is meant to serve as a starting point for those interested in applying either algorithm for verification.

The data-centric approach is completely non-intrusive, while the adjoint approach requires modifications to the model.

This is perhaps the most significant advantage for the data-centric approach. The fact that one needs to implement and solve an adjoint problem can be a non-starter. To state this another way, the data-centric verification process can be performed by anyone with access to the simulation output and knowledge of the discretizations used to generate the data. The adjoint approach requires

significant knowledge of the simulation environment to implement the adjoint problem and to compute the error representation. The implementation in Drekar::CFD uses a discrete adjoint approach which does not depend on the system of partial differential equations to be approximated (Navier Stokes, RANS, MHD, etc.), but it is subject to difficulties if the formulation is not adjoint consistent [5, 4].

The data-centric approach is applicable for a broader class of responses, e.g. maximum values.

While the adjoint-based approach can be extended to a certain class of nonlinear functionals, there are other classes of responses for which the adjoint problem is not easily defined. While this is an active area of research, to the best of our knowledge there is no solution for this.

The adjoint approach requires only one grid, while the data-centric approach requires at least three grids.

If the objective is to estimate the error for a particular discretization, then this is true. However, for robustness, the adjoint approach requires a higher order approximation of the adjoint solution which is roughly equivalent to solving a linear problem on a finer mesh. As previously mentioned, there are some postprocessing techniques that allow one to solve the adjoint on the same mesh, but these are not very robust. If one also wants to infer the convergence rate of the error, then at least two grids are required for the adjoint approach.

The data-centric approach can be applied to any number of quantities of interest, while the adjoint approach requires an adjoint solution for each $QofI$.

This is certainly an advantage for the data-centric approach. The computational cost for additional quantities of interest can be somewhat mitigated through the use of block-solvers since (for steady-state problems) this corresponds to solving the same linear systems with multiple right-hand sides. This capability has not been implemented in Drekar::CFD, but is the subject of future research.

The data-centric approach cannot distinguish between different sources of error, i.e., spatial and quadrature errors, and does not provide a local error indicator to be used for adaptive mesh refinement. Meanwhile, the adjoint approach provides a natural decomposition of errors into local contributions from various sources.

The ansatz for the data-centric approach can be modified to include interactions between different sources of error, but this does complicate the process and requires more parameters to be estimated. In section 0.3, we did not describe how the error representation can be decomposed into localized contributions from various sources of error, but this is fairly standard analysis and can be found in almost any text or journal article on adjoint-based error estimation. This ability to isolate local error contributions allows one to define local error indicators that may be used for adaptive mesh refinement.

The adjoint approach does not formally require the forward solution to be in the asymptotic regime and can provide accurate error estimates even on coarse meshes.

This is true if the adjoint solution can be approximated reasonably well. It is often claimed that the adjoint problem is *easier to solve* than the forward problem, but this is problem dependent. While the linearity of the adjoint problem certainly makes the discrete problem easier to solve, the adjoint solution itself may be more difficult to approximate than the solution of the forward problem, particularly if the solution to the forward problem is smooth enough to be given analytically. In section 0.5, we consider a case where the forward problem is much easier to solve than the adjoint problem, but nevertheless, the adjoint-based error estimate is still reasonably accurate.

Certain formulations do not have adjoints.

This is debatable. At the continuous level, most well-posed systems of PDEs have adjoints. However, it is often preferable to solve a discretized version of a modified problem. Examples include stabilized methods, LES models, etc. In such cases, there is no guarantee that the modified problem will have an adjoint. If this is the case, then one can always resort back to approximating the solution of the continuous adjoint, but this is much more intrusive than the discrete approach.

The simulation may have a systematic bias that causes the numerical approximation to converge to the incorrect answer. The adjoint-based approach may be able to detect this, while the data-centric approach will not.

The data-centric approach only determines whether or not a quantity of interest converges: it does not determine if it converges to the correct value. However, verification is process rather than an algorithm and the systematic biases that cause such false convergence are often due to implementation errors and should be culled out by performing verification on problems with known solutions or known quantities of interest.

The adjoint-based approach can be relatively difficult to implement correctly, and even minor mistakes can lead to inaccurate error estimates.

This is certainly true. The error representation must be implemented correctly in order to produce an accurate error estimate. Failing to do so typically results in an error estimate that does not account for all of the sources of error in the numerical approximation and may lead to false certification of the simulation. In section 0.5, we consider a case where this actually occurs and we describe the reason for the faulty error estimates.

The adjoint-based error estimate does not account for errors made in approximating the domain, while the data-centric approach includes this term.

For many practical problems, the computational domain is relatively complicated and cannot be matched exactly by the mesh. In such cases, there is an additional $\mathcal{O}(h^2)$ error induced by the approximation of the domain and it is difficult to determine a priori the relative magnitude of this error in comparison with other errors in the quantity of interest. The adjoint-based approach does not automatically account for this source of error and this may be the subject of future research.

0.5 Computational Experiments

0.5.1 Navier Stokes Channel Flow

In this section, we present numerical results for a two-dimensional laminar flow in a channel with an analytical solution. While this problem is rather simplistic, it does provide an opportunity to verify the adjoint solutions and the a posteriori error estimates. The computational domain is $[0, 5] \times [0, 1]$. Along the top and the bottom of the domain we enforce no-slip ($\mathbf{u} = \mathbf{0}$) boundary conditions. The flow for this problem is usually driven by specifying a parabolic profile for u_x along the inflow boundary. This introduces an additional error in the quantity of interest if we solve the forward problem using piecewise linear finite elements. The adjoint-based error estimate can account for this error adding a term of the form,

$$\int_{\Gamma} (-v \nabla \phi - q \mathbf{I}) \mathbf{n} (\mathbf{u} - \mathbf{u}_h) ds,$$

along the inflow boundary, where ϕ and q are the adjoint solutions corresponding to the velocity and pressure fields. This term is computable since \mathbf{u} is given on the boundary, but the straightforward implementation in `Drekar::CFD` does not include this term in the error representation.

Thus, we consider an alternative approach to drive the flow. The left and right boundaries are inflow and outflow boundaries respectively. The flow is driven by a forcing term,

$$\mathbf{g}_u = \begin{pmatrix} 1 \\ 0 \end{pmatrix},$$

which acts as a pressure gradient. This formulation has the same analytical solution as the standard formulation and the error estimate is fully computable in `Drekar::CFD`. The magnitude of the velocity vector for $v = 1E-2$ is shown in Figure 2. The x-velocity follows a parabolic profile, the y-velocity is zero, and the pressure is zero.

To discretize, we partition the computational domain into uniform quadrilateral (square) elements with mesh size h . The forward problem is solved using piecewise linear finite elements with SUPG and PSPG stabilization. The adjoint problem is solved using Algorithm 0.3.5 with piecewise quadratic finite elements. The adjoint data, $\boldsymbol{\psi}$, is determined by the quantity of interest. We use $\boldsymbol{\psi}_x$, $\boldsymbol{\psi}_y$, and $\boldsymbol{\psi}_z$ to denote the x, y, and z components of $\boldsymbol{\psi}$ respectively. Since u_y and the pressure field can be represented exactly in the finite element space we are only interested in errors in u_x , we consider the following quantities of interest associated with u_x for verification:

1. The value of the x-velocity at $(4, 1/2)$ for which

$$\boldsymbol{\psi}_x = \delta_{(4, 1/2)} \approx \frac{400}{\pi} \exp(-400(x-4)^2 - 400(y-1/2)^2).$$

2. The average value of the x-velocity over $[3, 4] \times [0, 1]$ for which

$$\boldsymbol{\psi}_x = \chi_{[3, 4] \times [0, 1]} = \begin{cases} 1, & (x, y) \in [3, 4] \times [0, 1], \\ 0, & \text{otherwise.} \end{cases}$$

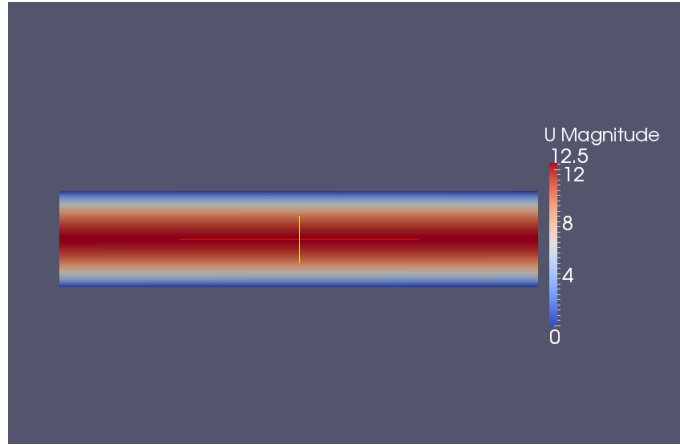


Figure 2. Magnitude of the forward velocity for the channel verification problem.

The exact values of the quantities of interest for the chosen Reynolds number are easily calculated to be

$$Q_1 = 12.405849827, \quad Q_2 = \frac{25}{3} \approx 8.333333333.$$

In Table 1, we provide the numerical approximations of the quantities of interest for a sequence of discretizations. Since the solution is known, we also provide the exact error for both quantities of interest on each mesh. It is clear from the data in Table 1 that the discretizations (except perhaps

h	Q_1	e_1	Q_2	e_2
1/10	12.2347875	0.1710623	8.25	0.0833333
1/20	12.3850150	0.0208348	8.3125	0.0208333
1/40	12.4006598	0.0051900	8.328125	0.0052083
1/50	12.4025300	0.0033198	8.33	0.0033333
1/80	12.4045561	0.0012937	8.33203125	0.0013021
1/100	12.4050237	0.0008261	8.3325	0.0008333
1/120	12.4052776	0.0005722	8.33275463	0.0005787
1/150	12.4054854	0.0003644	8.33296296	0.0003704

Table 1. Values of the quantities of interest for a sequence of discretizations.

the coarsest) are in the asymptotic regime and therefore both of the verification methods should perform quite well.

First, we use the data-centric verification approach to approximate the asymptotic value of the quantities of interest and the convergence rates. The constant C in (2) is also approximated but not reported here. As previously mentioned, we consider the standard metrics (L^2 , L^1 , L^∞ , weighted L^2) and perform regression on subsets of the data. The first subset contains the data from the three finest grids. Subsequent subsets are selected by adding data on coarser grids. For this data in Table 1, this results in 24 different regression results. The estimated convergence rates for the ensemble of regressions in shown in Figure 3 and the estimated asymptotic values of the quantities of interest are shown in Figure 4. We calculate the median of the predicted parameters,

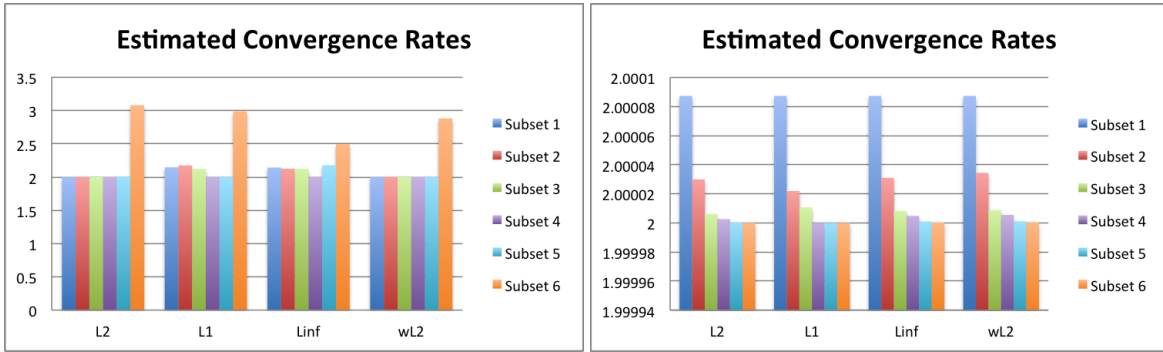


Figure 3. Estimated convergence rates for the ensemble of regressions for Q_1 (left) and Q_2 (right).

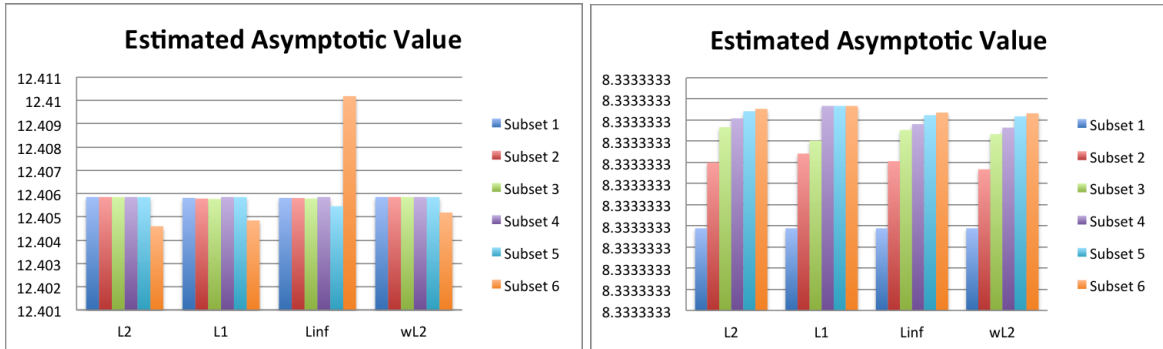


Figure 4. Estimated asymptotic values for the ensemble of regressions for Q_1 (left) and Q_2 (right).

Q_{median} and r_{median} and compute the median deviations, $\Sigma_{Q_{\text{median}}}$ and $\Sigma_{r_{\text{median}}}$. Following [17], we use $3\Sigma_{*,\text{median}}$ to approximate the bounds on the median values. This gives the following approximations for the asymptotic values

$$Q_1 = 12.405852538 \pm 7.906298999e-6, \quad r_1 = 2.004127413 \pm 0.016976748$$

$$Q_2 = 8.333333328 \pm 1.227539669e-8, \quad r_2 = 2.000005841 \pm 1.710263022e-5.$$

As expected, the median asymptotic rates and values of the quantities of interest are nearly exact and the error in the predicted values and the known values is well within the bounds provided. However, upon closer inspection of Figures 3 and 4, we see that the estimates are much worse for the sixth subset, which is the case that include all of the data points. It is quite likely that the coarsest mesh is unable to resolve Q_1 since the integral is approximated using quadrature. Therefore, we reanalyze the ensemble with the sixth subset omitted. This gives:

$$Q_1 = 12.405854693 \pm 3.637486989e-7, \quad r_1 = 2.000221938 \pm 8.936006080e-4.$$

Not only are the approximated values of the parameters closer to the known values, the bounds are much tighter. Omitting the sixth subset had a negligible effect on the estimates and bounds for Q_2 and r_2 .

Next, we use the adjoint-based approach to estimate the error for both quantities of interest on each mesh. Recall that this requires solving a higher-order, but linear, adjoint problem for each quantity of interest on each mesh. It is standard practice in a posteriori error estimation to report the *effectivity ratio*:

$$\text{Effectivity Ratio} = \frac{\text{Estimated Error}}{\text{True Error}},$$

as a measure of accuracy of the error estimate. Naturally, this is possible only if the true error is known. The a posteriori error estimates and effectivity ratios are provided in Table 2. As one might

h	e_1	Effectivity	e_2	Effectivity
1/10	7.70081e-2	0.45	8.33333e-2	1.00
1/20	2.07794e-2	0.99	2.08333e-2	1.00
1/40	5.19508e-3	1.00	5.20833e-3	1.00
1/50	3.32485e-3	1.00	3.33333e-3	1.00
1/80	1.29877e-3	1.00	1.30208e-3	1.00
1/100	8.31213e-4	1.01	8.33333e-4	1.00
1/120	5.77231e-4	1.01	5.78704e-4	1.00
1/150	3.69428e-4	1.01	3.70370e-4	1.00

Table 2. Values of the a posteriori error estimates and effectivity ratios for a sequence of discretizations.

expect, the effectivity ratios are very good for all simulations except for Q_1 on the coarsest mesh. As previously mentioned, this is probably due to the fact that the linear functional is not integrated very well on this mesh.

The a posteriori error estimate can be used to estimate the asymptotic value of the quantities of interest by adding the error to the approximation. In Figure 5, we plot the approximated asymptotic values and we see that all of the approximations are quite good except for Q_1 on the coarsest mesh.

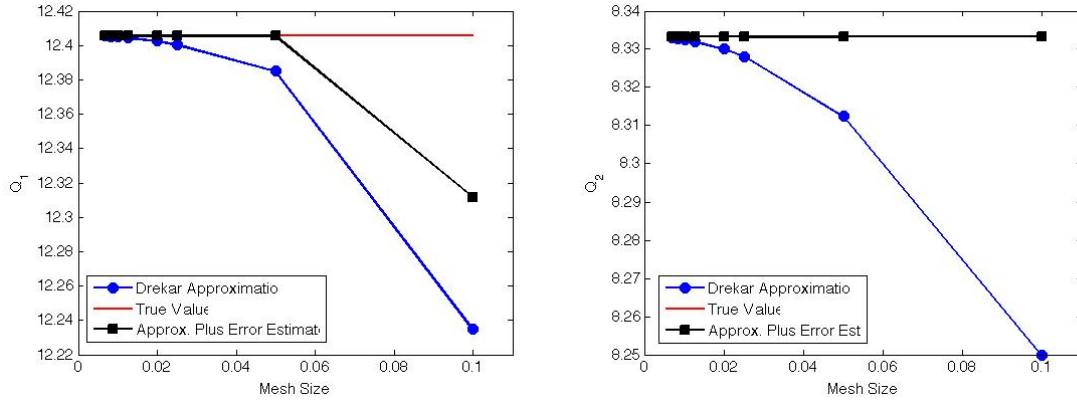


Figure 5. Approximate values of the quantities of interest as well as the sum of the approximations and the error estimates for Q_1 (left) and Q_2 (right).

The adjoint-based approach only provides an estimate of the error in a quantity of interest on a given mesh. It does not provide bounds or estimates of the error in the error estimate. However, we could treat the predicted asymptotic values and error estimates as *additional data* and combine the data-centric and adjoint-based approaches to estimate the asymptotic rate of convergence of the error and to provide bounds on the estimates. For the asymptotic values, we could then add the numerical approximations of the quantities of interest in Table 1 and the error estimates in Table 2 and perform the ensemble of regressions on the sum. Unfortunately, the data from Drekar::CFD was provided with *only* seven digits of accuracy, and while this usually sufficient, the error in the sum is well below this threshold for most of the discretizations. Thus, there is a systematic bias in the data and the regressions perform quite poorly. Of course, one would not expect to encounter this issue when dealing with more practical problems.

We can still combine the data-centric and adjoint-based approaches to estimate the rates of convergence. We start with the ansatz,

$$e = Ch^r + \text{higher order terms} ,$$

and perform an ensemble of regressions on the data in Table 2. This gives the following approximations for the convergence rates:

$$r_1 = 1.999999567 \pm 1.866173069e-6. \quad r_2 = 2.000000235 \pm 2.334115517e-6,$$

which are nearly exact to within the precision of the data and the bounds reflect the accuracy in the data. We also computed the medians with the data from the coarsest mesh omitted, but this had a negligible effect on the results.

0.5.2 RANS Model for Axisymmetric Expansion

In this section, we consider the axisymmetric sudden expansion problem (Benchmark #2 from TH-M). The computational domain consists of two cylinders of different radii as shown in Figure 6. The flow is in the z-direction and we do not consider the case with swirl.

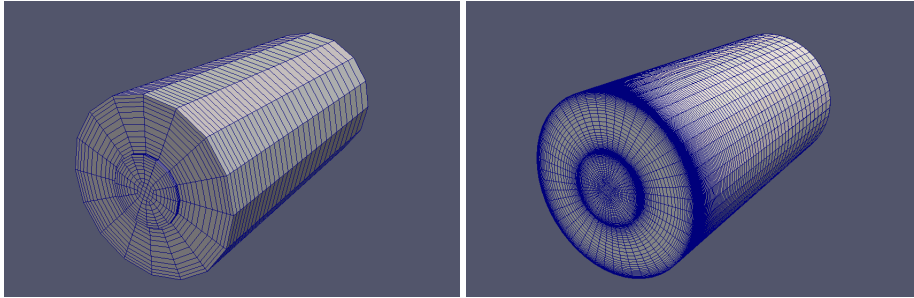


Figure 6. Coarsest (left) and finest (right) computational meshes for the axisymmetric sudden expansion problem.

Mesh Number	Elements	Nodes
1	10656	11307
2	35964	37396
3	80896	83349
4	166500	170406
5	287712	293311

Table 3. Number of nodes and elements on each of the five meshes.

We use a Reynolds Averaged Navier Stokes (RANS) model to approximate a steady solution to the problem described above at a Reynolds number of about 2500. We use a Spalart-Allmaras RANS model which requires the solution of a time-dependent advection-diffusion-reaction equation to approximate the turbulent viscosity. We solve the forward problem using a stabilized continuous Galerkin method with piecewise linear basis functions. The adjoint problem is solved using Algorithm 0.3.5 and uses piecewise quadratic basis functions. The significant increase in degrees of freedom for the adjoint problem did not pose a problem for the linear solver since the physics based algebraic multigrid preconditioner performed well in all simulations. The main challenge in solving the adjoint problem was due to the increased memory requirements to assemble and store the adjoint Jacobian which was much denser than the Jacobian of the forward problem. Thus,

all of the numerical results were obtained using the Redsky capacity machine at Sandia National Laboratories on between 128 and 2048 cores.

We integrate the forward problem in time until $t = 50$ at which point a steady state has been reached. In fact, a steady state is reached a bit earlier, but we perform additional time stepping to insure that all of the transient are removed from the solution. Then we solve the steady state adjoint and compute an a posteriori error estimate using Algorithm 0.3.5. For this particular problem, the fact that we need to solve a time-dependent forward problem and a steady-state adjoint problem actually renders the total solution time for the adjoint problem about an order of magnitude less than the solution time for the forward problem, despite the use of the higher-order basis functions.

In the first experiment, we prescribe a uniform inflow velocity, $\mathbf{u}_z = 1$ on the inflow of the smaller tube. No-slip boundary conditions ($\mathbf{u} = \mathbf{0}$) are imposed on all other boundary except the outflow of the larger tube where a natural outflow condition is chosen. We consider the following quantities of interest associated with u_z for verification:

1. The value of the z-velocity near $(0.0450, 0.1)$ for which

$$\psi_z = 3100 \exp(-400(x - 0.045)^2 - 400(y)^2 - 400 * (z - 0.1)^2).$$

2. The average value of the z-velocity over the entire domain for which

$$\psi_z = \frac{1}{|\Omega|}.$$

3. The average value of the z-velocity for $0.18 \leq z \leq 0.2$ for which

$$\psi_z = \begin{cases} \frac{1}{0.02(\pi 0.05^2)}, & 0.18 \leq z \leq 0.2, \\ 0, & \text{otherwise.} \end{cases}$$

The numerical approximations of these quantities of interest are reported in Table 4. A quick

Mesh Number	Q_1	Q_2	Q_3
1	1.44020926e-1	1.50579962e-1	1.59236405e-1
2	1.49755223e-1	1.55737659e-1	1.62925617e-1
3	1.50095835e-1	1.55827310e-1	1.52577120e-1
4	1.53843384e-1	1.59340034e-1	1.51289017e-1
5	1.54736999e-1	1.60150819e-1	1.69128152e-1

Table 4. Values of the quantities of interest for a sequence of discretizations using a prescribed inflow velocity.

inspection of the data would indicate that Q_1 and Q_2 may be converging, but probably not Q_3 . Nevertheless, we perform an ensemble of regressions on all three quantities of interest and compute the

median asymptotic values and convergence rates as well as the median deviation for each quantity of interest. Since this problem is more challenging than the laminar Navier Stokes example, we perform a constrained optimization where we restrict the convergence rate to within the interval $[0.25, 2]$. This gives:

$$Q_1 = 1.59240880e-1 \pm 1.02994326e-2, \quad r_1 = 1.05414626 \pm 0.34630880,$$

$$Q_2 = 1.63998250e-1 \pm 9.04053287e-3, \quad r_2 = 1.08317760 \pm 0.55660220,$$

$$Q_3 = 1.60363486e-1 \pm 3.92977461e-3, \quad r_3 = 0.86072531 \pm 0.22793075.$$

The estimated convergence rates and asymptotic values for each ensemble member are provided in Figure 7 and Figure 8 respectively. Quite surprisingly, the median convergence rates are very close

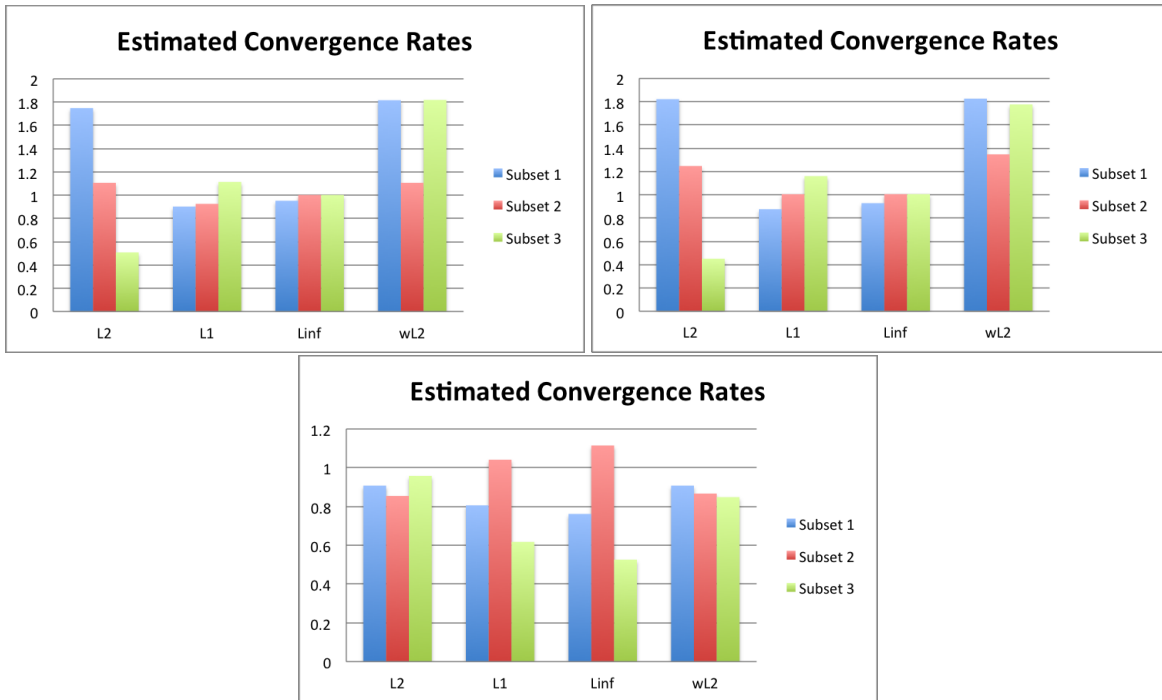


Figure 7. Estimated convergence rates for the ensemble of regressions for Q_1 (upper-left), Q_2 (upper-right), and Q_3 (lower-middle).

to the anticipated value of 1 despite the fact that there are several outliers within the ensemble. In contrast to the results in the previous section, no particular subset appears to be causing the outliers. The variation in the predicted values is reflected in the relatively large bounds for the convergence rates.

Next, we solve the adjoint problem for each quantity of interest and report the a posteriori error estimates in Table 5. At first glance, the error estimates appear to be converging at a reasonable

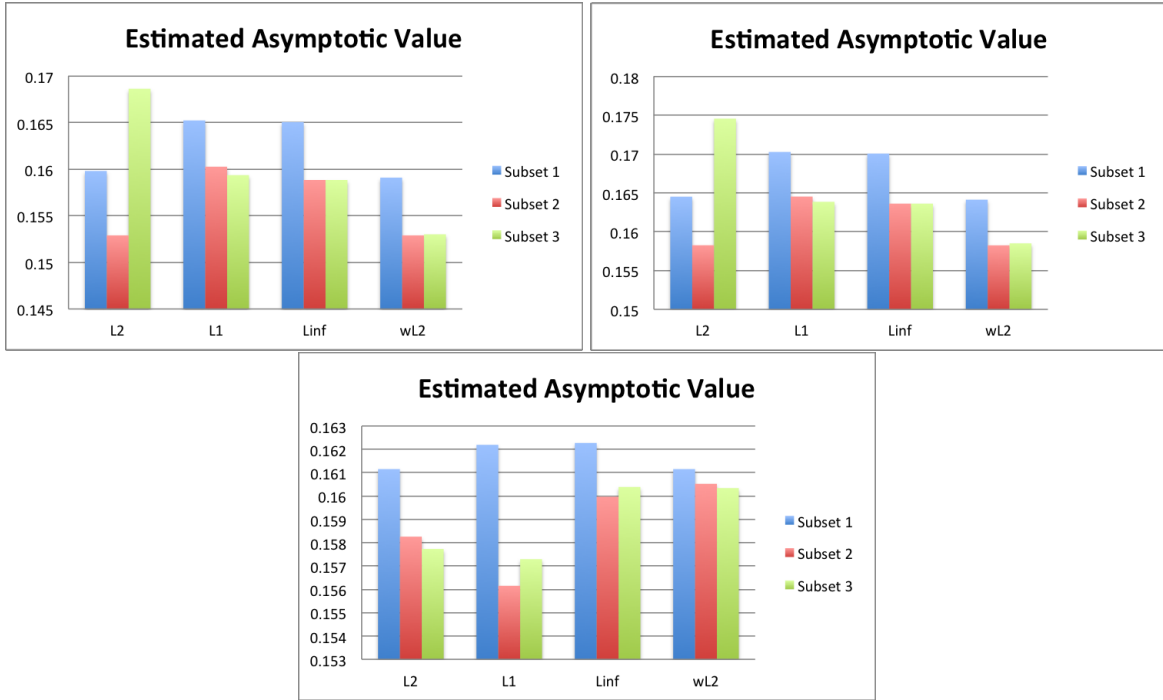


Figure 8. Estimated asymptotic values for the ensemble of regressions for Q_1 (upper-left), Q_2 (upper-right), and Q_3 (lower-middle).

Mesh Number	e_1	e_2	e_3
1	-1.73453e-3	-9.24103e-5	-9.16013e-3
2	-1.33005e-3	-3.74300e-5	-2.73042e-3
3	-1.44005e-3	-2.46298e-5	-1.74194e-3
4	-6.14935e-4	-1.27056e-5	-1.15997e-3
5	-4.18171e-4	-8.70172e-6	-1.95917e-4

Table 5. Values of the error estimates for a sequence of discretizations using a prescribed inflow velocity.

rate. Performing an ensemble of regressions gives the following estimates for the convergence rates of the error:

$$\begin{aligned}
 r_{e_1} &= 1.41747878 \pm 1.18095318, \\
 r_{e_2} &= 2.10054191 \pm 0.34524074, \\
 r_{e_3} &= 2.61035252 \pm 1.04263704.
 \end{aligned}$$

Note that we did not constrain the optimization algorithm since the errors appear to be converging. However, we also notice that the magnitude of the error estimate is much smaller than the magnitude of the variation in the data. Moreover, the predicted convergence rate is much higher, albeit with larger bounds. This indicates that there is probably a component of the error that the a posteriori error estimate is not accounting for. For this particular problem, there are several potential sources for this additional error. One issue is due to the inflow boundary where we set $u_z = 1$ on the inflow face and we set $u_z = 0$ on the side of the smaller cylinder. This introduces an error in the interpolation of the boundary conditions since the nodes common to both boundaries can be *either* 0 or 1.

To mitigate this issue, we modify the problem to be driven by a pressure gradient rather than a prescribed inflow velocity. We set the pressure gradient so that the Reynolds number is fairly close to the previous case. In Table 6, we provide the numerical approximations of the three quantities of interest on each mesh.

Mesh Number	Q_1	Q_2	Q_3
1	1.19399798e-1	1.25705177e-1	1.30725526e-1
2	1.26371320e-1	1.32560106e-1	1.38197096e-1
3	1.30495505e-1	1.36662326e-1	1.33800602e-1
4	1.21417426e-1	1.27037231e-1	1.20816139e-1
5	1.22591353e-1	1.28248290e-1	1.35645515e-1

Table 6. Values of the quantities of interest for a sequence of discretizations using a pressure drop to drive the flow.

We perform the same ensemble of regressions which gives

$$Q_1 = 1.25079995e-1 \pm 1.69518368e-3, \quad r_1 = 0.95816574 \pm 0.37831641,$$

$$Q_2 = 1.30984086e-1 \pm 1.34550707e-3, \quad r_2 = 0.96170827 \pm 0.26145869,$$

$$Q_3 = 1.28348004e-1 \pm 7.45314446e-4, \quad r_3 = 0.87331692 \pm 0.30038723.$$

The estimated convergence rates and asymptotic values for each ensemble member are provided in Figure 9 and Figure 10 respectively. While the asymptotic values of the quantities of interest are different due to the modified formulation of the problem, the estimated convergence rates and the error bounds are comparable to the previous case.

Next, we solve the adjoint problem for each quantity of interest on each mesh and report the a posteriori error estimates in Table 7. These error estimates certainly appear more reasonable, but it is evident that there might be another source of error that the adjoint-based estimate is missing. In Section 0.4, we noted that the adjoint-based error estimate is unable to account for errors due to approximations of the geometry. It is possible that the error estimate is only capturing the

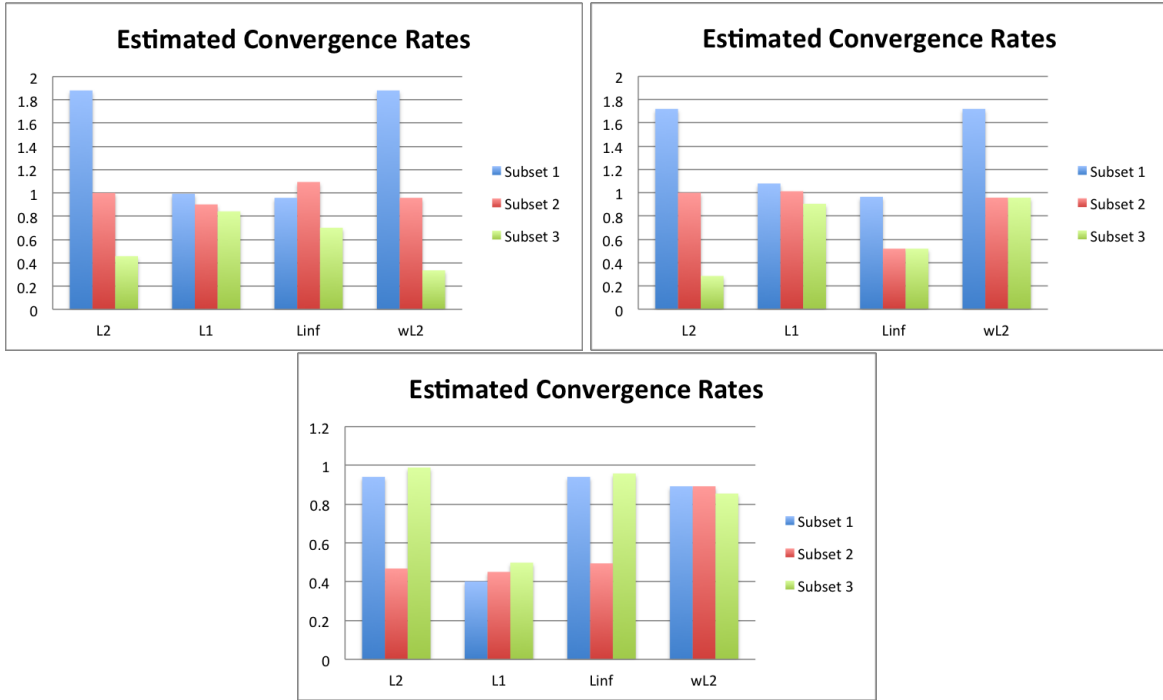


Figure 9. Estimated convergence rates for the ensemble of regressions for Q_1 (upper-left), Q_2 (upper-right), and Q_3 (lower-middle).

Mesh Number	e_1	e_2	e_3
1	-6.26274e-2	-6.672304e-2	-6.92621e-2
2	-1.67401e-2	-1.762705e-2	-1.83955e-2
3	-1.92805e-2	-2.033776e-2	-1.99137e-2
4	-1.28515e-3	-1.330209e-3	-1.31282e-3
5	-1.24453e-3	-1.293814e-3	-1.29362e-3

Table 7. Values of the error estimates for a sequence of discretizations using a prescribed inflow velocity.

discretization errors and missing the geometrical errors. Another possibility, also mentioned previously, is that using the adjoint of the SARANS model is causing an instability in the discrete adjoint problem. Finally, we note that the numerical approximation does not appear to be in the asymptotic range, which might be also affecting the a posteriori error estimate. All of these possibilities will need to be investigated in the future.

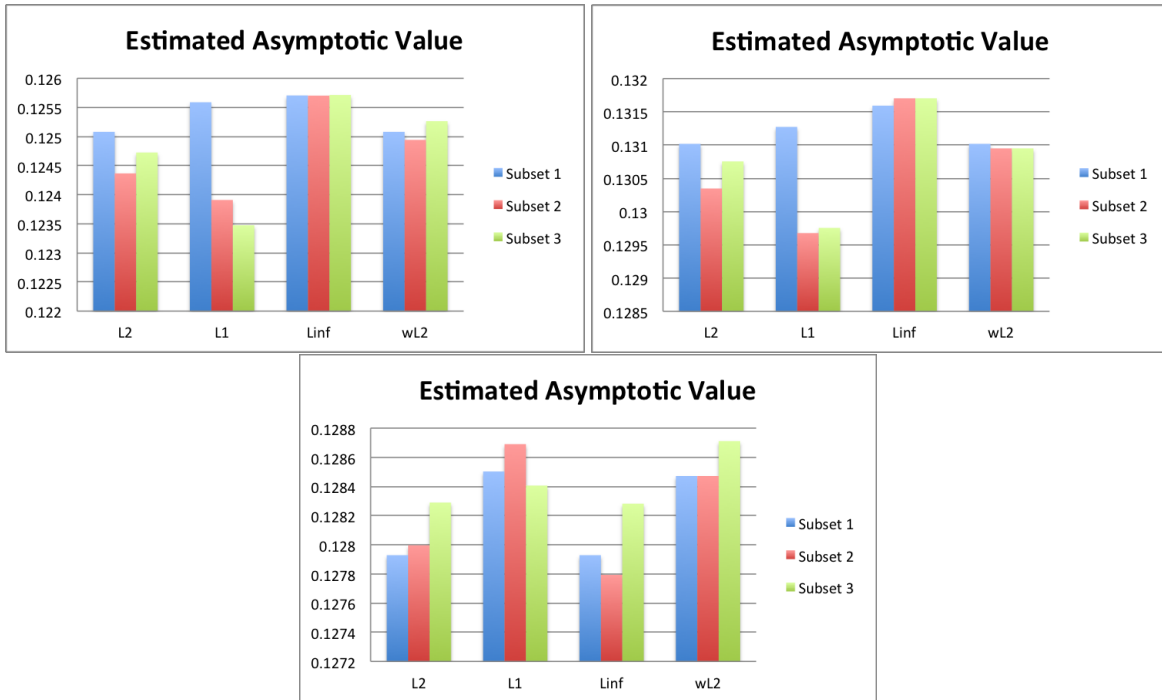


Figure 10. Estimated asymptotic values for the ensemble of regressions for Q_1 (upper-left), Q_2 (upper-right), and Q_3 (lower-middle).

0.6 Conclusions

Our objective in this report was to provide a brief overview of the adjoint-based and data-centric verification techniques and to give a summary of their respective advantages and disadvantages. We showed that in the case of a numerical solution within the asymptotic range of convergence, both methods performed quite well and were even complementary in the sense that data-centric technique can be applied to the a posteriori error estimates to yield extremely accurate convergence rates and tight bounds. We also showed that for more challenging problems where the solution is away from the asymptotic range, both methods may struggle. In the data-centric approach, the result is relatively wide bounds on the predicted quantities of interest and convergence rates. For the adjoint-based approach, the result is unreliable error estimates. Nevertheless, both approaches are reasonable in a range of scenarios and the fact that they can even be combined to make more precise bounds and estimates is a promising avenue for future research.

References

- [1] W. Bangerth and R. Rannacher. *Adaptive Finite Element Methods for Differential Equations*. Birkhauser Verlag, 2003.
- [2] Roland Becker and Rolf Rannacher. An optimal control approach to a posteriori error estimation in finite element methods. *Acta Numer.*, 10:1–102, 2001.
- [3] V. Carey, D. Estep, and S. Tavener. *A posteriori* analysis and adaptive error control for multiscale operator decomposition solution of elliptic systems I: Triangular systems. *SIAM J. Numer. Anal.*, (47):740–761, 2009.
- [4] S.S. Collis and M. Heinkenschloss. Analysis of the streamline-upwind/petrov-galerkin method applied to the solution of optimal control problems. Technical Report TR02-01, Department of Computational and Applied Mathematics, Rice University, Houston, TX 77005-1892, 2002.
- [5] E. Cyr, J. Shadid, and T. Wildey. Approaches for adjoint-based a posteriori analysis of stabilized finite element methods. Submitted to *SIAM J. Sci. Comp.*, 2012.
- [6] K. Eriksson, D. Estep, P. Hansbo, and C. Johnson. *Computational differential equations*. Cambridge University Press, Cambridge, 1996.
- [7] D. Estep. A posteriori error bounds and global error control for approximation of ordinary differential equations. *SIAM J. Numer. Anal.*, 32(1):1–48, 1995.
- [8] D. Estep, V. Ginting, J. Shadid, and S. Tavener. An a posteriori-a priori analysis of multiscale operator splitting. *SIAM J. Numer. Anal.*, 46:1116–1146, 2008.
- [9] D. Estep, M. G. Larson, and R. D. Williams. Estimating the error of numerical solutions of systems of reaction-diffusion equations. *Mem. Amer. Math. Soc.*, 146(696):viii+109, 2000.
- [10] D. Estep, S. Tavener, and T. Wildey. *A posteriori* analysis and improved accuracy for an operator decomposition solution of a conjugate heat transfer problem. *SIAM J. Numer. Anal.*, 46:2068–2089, 2008.
- [11] D. Estep, S. Tavener, and T. Wildey. A posteriori error estimation and adaptive mesh refinement for a multiscale operator decomposition approach to fluid-solid heat transfer. *J. Comput. Phys.*, 229:4143–4158, June 2010.
- [12] K. Harriman, D. Gavaghan, and E. Suli. The importance of adjoint consistency in the approximation of linear functionals using the discontinuous galerkin finite element method. Technical report, Oxford University Computing Laboratory, Oxford, 2004.

- [13] Ralf Hartmann. Adjoint consistency analysis of discontinuous galerkin discretizations. *SIAM J. Numer. Anal.*, 45:2671–2696, October 2007.
- [14] Michael Heroux, Roscoe Bartlett, Vicki Howle Robert Hoekstra, Jonathan Hu, Tamara Kolda, Richard Lehoucq, Kevin Long, Roger Pawlowski, Eric Phipps, Andrew Salinger, Heidi Thornquist, Ray Tuminaro, James Willenbring, and Alan Williams. An Overview of Trilinos. Technical Report SAND2003-2927, Sandia National Laboratories, 2003.
- [15] William L. Oberkampf and Christopher J. Roy. *Verification and Validation in Scientific Computing*. Cambridge University Press, 2010.
- [16] William L. Oberkampf and Timothy G. Trucano. Verification and Validation in Computational Fluid Dynamics. Technical Report SAND2002-0529, Sandia National Laboratories, 2002.
- [17] William J. Rider and James R. Kamm. Advanced Solution Verification of CFD Solutions for LES of Relevance to GTRF Estimates. Technical Report SAND2012-7199P, Sandia National Laboratories, 2012.
- [18] P. J. Roache. *Verification and Validation in Computational Science and Engineering*. Hermosa, Albuquerque N. M., 1998.
- [19] Timothy M. Wildey, Eric C. Cyr, Roger Pawlowski, John N. Shadid, and Tom M. Smith. Adjoint Based a posteriori Error Estimation in Drekar::CFD. Technical Report SAND2012-8910, Sandia National Laboratories, 2012.
- [20] Tao Xing and Frederick Stern. Factors of safety for richardson extrapolation. *Journal of Fluids Engineering*, 132(061403):1 – 13, 2020.

DISTRIBUTION:

1	MS 1318	Brian M. Adams, 1441
3	MS 1318	Michael S. Eldred, 1441
1	MS 1318	James R. Stewart, 1441
3	MS 1318	Timothy M. Wildey, 1441
1	MS 1320	Eric C. Cyr, 1426
1	MS 1320	Thomas M. Smith, 1442
1	MS 1321	John N. Shadid, 1444
1	MS 1323	William J. Rider, 1443
1	MS 1318	Roger P. Pawlowski, 1444
1	MS 1318	James R. Kamm, 1441
1	MS 0899	Technical Library, 9536 (electronic copy)

